



HHS Public Access

Author manuscript

J Comput Chem. Author manuscript; available in PMC 2019 November 26.

Published in final edited form as:

J Comput Chem. 2019 June 30; 40(17): 1622–1632. doi:10.1002/jcc.25813.

***Stalis*: A Computational Method for Template-based Ab Initio Ligand Design**

Hui Sun Lee^{*}, Wonpil Im^{*}

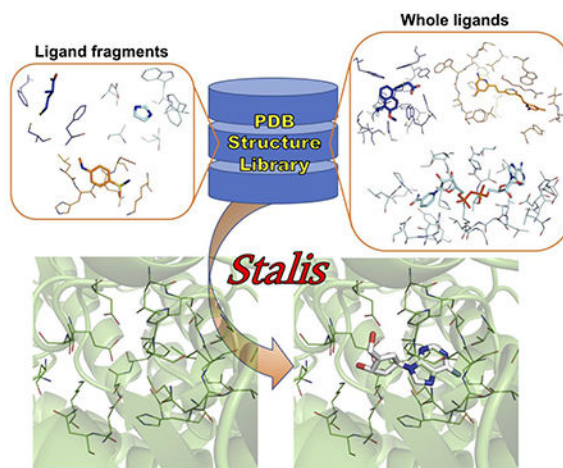
Departments of Biological Sciences and Bioengineering, Lehigh University, 111 Research Drive, Bethlehem, PA 18015, USA

Abstract

Proteins interact with small molecules through specific molecular recognition, which is central to essential biological functions in living systems. Therefore, understanding such interactions is crucial for basic sciences and drug discovery. Here, we present *Stalis* (Structure template-based ab initio ligand design solution), a knowledge-based approach that uses structure templates from the PDB libraries of whole ligands and their fragments and generates a set of molecules (virtual ligands) whose structures represent the pocket shape and chemical features of a given target binding site. Our benchmark performance evaluation shows that ligand structure-based virtual screening using virtual ligands from *Stalis* outperforms a receptor structure-based virtual screening using AutoDock Vina, demonstrating reliable overall screening performance applicable to computational high-throughput screening. However, virtual ligands from *Stalis* are worse in recognizing active compounds at the small fraction of a rank-ordered list of screened library compounds than crystal ligands, due to the low-resolution of the virtual ligand structures. In conclusion, *Stalis* can facilitate drug discovery research by designing virtual ligands that can be used for fast ligand structure-based virtual screening. Moreover, *Stalis* provides actual three-dimensional ligand structures that likely bind to a target protein, enabling to gain structural insight into potential ligands. *Stalis* can be an efficient computational platform for high-throughput ligand design for fundamental biological study and drug discovery research at the proteomic level.

Graphical Abstract

^{*}To whom correspondence should be addressed: huisun@lehigh.edu; wonpil@lehigh.edu.



Abstract

A better understanding of protein-ligand interactions in the context of their three-dimensional structure is essential for fundamental biological study and structure-based drug discovery. We present *Stalis*, a knowledge-based computational method that uses structure templates from the Protein Data Bank to design small molecule ligands for a given target protein. This method provides actual protein-bound ligand structures. Our benchmark performance evaluation also demonstrates the reliable quality of the computationally designed ligands for fast ligand structure-based virtual high-throughput screening.

Keywords

protein-ligand interaction; template-based approach; computer-aided drug discovery; virtual screening; fragment-based drug design

Introduction

One of the most remarkable features of proteins is their ability of specific, reversible binding to other molecules (i.e., other proteins, small molecules, carbohydrates, lipids, or nucleic acids). Of greatest importance is the fact that these molecular recognitions are associated with a vast array of essential biological functions in living systems. Many proteins interact with small molecule ligands, such as cofactors, metabolites, neurotransmitters, and hormones. Therefore, accurate characterization of these endogenous ligands that bind to specific proteins is crucial to better understand protein functions. For example, metabolites serve as signals to control a variety of cellular processes mainly to maintain cellular homeostasis through either orthosteric or allosteric interactions.^[1–3] In addition to such fundamental biology studies, interactions between proteins and small molecules are a vital consideration in the development of new drugs.

Researchers have been trying to probe ligands that specifically bind to a target protein. Global mass spectrometry approaches are used to identify endogenous ligand(s) to a given protein from a large pool of metabolites.^[4] In this approach, an immobilized protein of

interest is incubated with a metabolite mixture and a bound-metabolite to the target protein is analyzed using a liquid chromatography-mass spectrometry (LC-MS). In pharmaceutical industry, high-throughput screening (HTS) is a routine approach to the identification of small molecules that selectively bind to a target protein.^[5] An HTS campaign screens considerable numbers of compounds (usually up to 10^6 molecules), but these compound libraries still have limitation of fully covering possible chemical space. To tackle this problem, fragment-based drug design (FBDD) is used to find small molecules that bind to target protein as a complementary and contrasting approach to HTS.^[6] In this approach, a smaller library consisting of fragment molecules (<300 Da) is screened in vitro using an array of biophysical techniques and then the validated fragment hits are synthetically elaborated into larger molecules for better affinity. Once a hit molecule is obtained from diverse experimental approaches including LC-MS, HTS, and FBDD, people seek to solve the three-dimensional (3D) structure of the protein-ligand complex by biophysical techniques such as X-ray crystallography and nuclear magnetic resonance (NMR) to determine a bioactive conformation of the ligand and the detailed atomic interactions between the ligand and protein. Although these experimental approaches provide valuable information to identify protein-small molecule interactions, they require significant investment in equipment and are often time-consuming. In recent years, moreover, the productivity decline in pharmaceutical research and development, despite of huge advances in sciences and technologies, is urging to develop alternative approaches to improve efficiency in drug discovery.^[7]

In the efforts to solve this problem, computational methods have emerged to predict endogenous ligands and to aid design and optimize new molecules to modulate protein functions. Given the 3D protein structure of a target protein, molecular docking is a common method of choice to predict small molecules (from compound libraries) that likely bind to the protein.^[8] The docking computationally fits molecules by changing their conformations and positions and evaluate their binding affinities using a given scoring function. More than 60 different docking tools are currently available for both academic and commercial use,^[9] such as GOLD,^[10] ICM,^[11] Surflex,^[12] Glide,^[13] AutoDock Vina,^[14] and DOCK6.^[15] Although molecular docking is a critical component in current drug discovery campaigns, the inaccuracy in scoring functions and the sensitivity of docking results to marginal conformational changes in ligand binding sites significantly reduce the chances of finding correct ligands.^[16,17] Furthermore, performing docking calculations with vast number of compounds is still computationally expensive.

In silico FBDD tools serve as a complementary method to the molecular docking. While docking relies on pre-existing compounds, this approach generate molecules by identifying building blocks (fragments) within a target binding site and linking them (i.e., ab initio approach).^[18] The applicability of this approach, however, is limited mainly by low efficiency in the sampling of the chemical space and poor accuracy of scoring functions. With a rapid increase in the number of high-resolution protein structures in the Protein Data Bank (PDB, <http://www.rcsb.org>),^[19] structural information from known protein-ligand structures can be used to design small molecule ligands. Our previous study indicates that similar binding sites occur in unrelated protein structures, making it feasible to predict ligand structures from protein-ligand complex structures in the PDB.^[20–22] As an example

of this knowledge-based approach, a commercial tool, MED-Portion/MED-SuMo/MED-Hybridise detects MED-Portions, protein-fragment binding sites that are derived from the PDB protein-ligand complex structures by MED-SuMo and generate a pool of MED-Portion hybrids by MED-Hybridise.^[23] PoLi is a computational pipeline for virtual screening.^[24] PoLi first predicts the ligand-binding pocket in a target protein and copies template ligands based on binding-pocket alignment by APoc. Up to the top 200 copied template ligands are subject to virtual screening against a compound library based on two-dimensional (2D) and 3D ligand similarity metrics.

In this study, we present a knowledge-based approach, *Stalis* (Structure template-based ab initio ligand design solution). *Stalis* is a template-based computational method to design small molecule ligands for a given target binding site. In our previous study, we have developed an efficient local structure alignment tool, G-LoSA (Graph-based Local Structure Alignment; <https://compbio.lehigh.edu/GLoSA>).^[22] A recent comprehensive benchmark performance evaluation study reports that G-LoSA offers a fairly robust overall performance over other widely used local structure alignment tools.^[25] *Stalis* is developed to design ligands by harnessing structure templates identified by G-LoSA from the PDB structure libraries of small molecule ligands and their chemical fragments. We first describe the algorithm of *Stalis*. Comprehensive benchmark performance evaluation tests are then presented to validate the applicability of *Stalis* to ligand structure-based virtual screening. Representative examples of the ligands designed by *Stalis* are illustrated, followed by discussion on its potential for biological study and structure-based drug design.

Methods

Improvements of G-LoSA

G-LoSA is a computational tool to align protein local structures in a sequence order independent way and to provide a GA-score (G-LoSA Alignment score), a size-independent quantity of structural similarity for a given structure pair.^[22] G-LoSA generates possible structure alignments between two structures by iterative maximum clique search and fragment superposition based on the geometry of C α atoms (i.e., single-point representation of each residue). The GA-score is a scoring function to quantify structural similarity based on the chemical feature points (CFPs) of each amino acid (i.e., multiple CFPs for each residue). GA-score is defined as

$$\text{GA-score} = \text{Max} \left[\frac{1}{N_T} \left(\sum_i^{N_{\text{ali}}} \frac{q_i}{1 + \left(\frac{d_i}{d_0(N_T)} \right)^2} \right) \right] \quad (1)$$

where ‘Max’ denotes that the GA-score is the maximum of all possible alignments, N_T is the smaller number of CFPs between two local structures, and N_{ali} is the number of aligned CFPs. d_i is the distance between the CFPs in the i th pair. $d_0(N_T)$ is a size-dependent scaling factor to normalize the aligned distances. q_i is defined based on the chemical feature similarity of the i th CFP pair.

This hybrid approach (i.e., alignment by C α atoms and scoring by CFPs) has been designed to achieve a reliable measurement of structural similarity with high computing efficiency. However, this approach fails to generate good alignments between two structures that do not have any significant conservation of their C α atoms, but do have highly conserved side chain CFPs. To tackle this problem, we have modified the iterative maximum clique search algorithm to generate additional initial alignments based on CFPs (CFP-based iterative maximum clique search). Although using CFPs is computationally more expensive due to the larger number of representing points, the cost can be offset by the smaller size of ligand fragment binding site. A representative example is shown in Figure S1 to demonstrate the effect of the CFP-based iterative maximum clique search in improving the quality of local structure alignment by G-LoSA.

To validate the size-independency of GA-score by the updated G-LoSA, we generated 18,270 random ligand binding site patches using the ligand-containing PDB structures (as of Feb. 2016, resolution 3 Å) and performed all-to-all G-LoSA alignments, showing that mean GA-scores are independent of the number of CFPs (Figure S2). The GA-score distribution modeled by the type I extreme value distribution indicates that a GA-score of 0.52 is significant at $P < 5 \times 10^{-2}$ (Figure S3).

Generation of PDB ligand/binding-site structure library

We downloaded all PDB entries containing at least one protein and one ligand whose resolution is better or equal to 3.5 Å from the PDB.^[19] DNA and RNA molecules were discarded, and ligand molecules in the PDB files were identified in the heteroatom section. Heteroatoms having an identical chain ID and sequence number were grouped into one heteroatom group. If a distance of any atom pair from different heteroatom groups was 1–2 Å, the two heteroatom groups were merged into one group and identified as multipart ligands. Small molecular weight additives were removed by setting the minimum number of heavy atoms in a heteroatom group to 5. Metal ions and water molecules were saved as separate files. If any atom of a protein residue is within 4.5 Å of its cognate ligand, the residue is defined as the binding-site residue. Metal- and water-mediated interactions were defined by the cutoff distances of 3.0 Å and 3.2 Å from any ligand and protein atom, respectively. The protein residues involved in the metal- and water-mediated interactions were also added to the binding-site residues. Homologous binding-sites were removed by sequence identity $\geq 70\%$ between the protein chains using BLAST clustering results (<ftp://resources.rcsb.org/sequence/clusters/>). A binding site from a PDB structure with worse resolution was removed from a pair of homologous binding sites. If two binding sites are homologous and their ligands are not identical, both binding sites were kept in the structure library. A path-based fingerprint (FP2 option) using 1024-bit vector in Open Babel (version 2.4)^[26] was used to measure the structural similarity between ligands. There were 79,710 ligand/binding-site structure pairs in this PDB structure library (as of July, 2018).

Generation of PDB ligand fragment/binding-site structure library using MolFrag

To construct a PDB structure library of ligand fragments and their binding sites, we have developed *MolFrag* to automatically dissect PDB ligands into chemical fragments and then identify their binding sites. Sequential steps for ligand fragmentation in *MolFrag* are

outlined in Figure S4. *MolFrag* first detects rings in a given PDB ligand using an exhaustive ring perception algorithm by Hanser *et al*, which is based on a progressive collapsing of the path graph.^[27] Based on the ring structures identified by this algorithm, a PDB ligand is divided into rings, substituents, and linkers. A linker is a chemical group whose two ends are connected to rings. A substituent is a chemical group with only one end connected to a ring. Each ring, substituent, or linker is assigned as a fragment. Substituent fragments with < 3 atoms are merged with their linked rings. Specific chemical groups (e.g., CO₂, PO₄, SO₄) in a substituent or linker fragment (with > 5 atoms) that can favorably interact with receptor are separated from their fragment and assigned as new fragments. Chemical groups such as -CO-, -CN-, -CS- in a linker with > 5 atoms are also assigned as separate fragments. In addition, an atom with the largest number of linkages is detected from a substituent or linker, and then the atom and its linked atoms are assigned as a separate fragment. This procedure is iterated until there is no atom with ≥ 2 linkages. Lastly, the continuity of atom linkages is checked in each fragment and a discontinuous fragment is separated at the broken points. A ligand with no ring structure is fragmentized as a whole using the same algorithm. Fragmentation of a PDB ligand by *MolFrag* is shown in Figure 1 as an example.

A workflow of generating a PDB binding-site library using the ligand fragments generated using *MolFrag* is shown in Figure 2. If a fragment has < 3 atoms, the fragment is merged with its smallest adjacent fragment. This process is iterated until there is no fragment with < 3 atoms. Binding-site residues are identified for each ligand fragment by *MolFrag* using the cutoff distances. If a ligand fragment has its binding site with < 5 residues, an adjacent ligand fragment with the smallest number of binding-site residues is identified, and the two ligand fragments and their binding sites are merged. This procedure is iterated until there is no ligand fragment binding site with < 5 residues. The procedure of binding-site identification for the ligand fragments by *MolFrag* in Figure 1 is illustrated in Figure 3.

SLIM-score

SLIM (Shape-based Ligand Matching with binding pocket) is a high-speed virtual screening method to generate receptor-ligand complex models and evaluate their relative binding affinity quantified by the SLIM-score.^[17,28] The SLIM-score is a coarse-grained approach to approximately measure relative binding affinity by calculating shape and chemical feature complementarity between each library compound and the negative image of a binding pocket that is a set of virtual atoms representing the inner shape and chemical features of the binding pocket.

To generate the negative image of each target protein, a box centered by its cognate ligand with the size of 30 Å for X, Y, and Z was divided into a set of grid points using a grid spacing of 2 Å. To specifically extract the inner shape of a binding pocket, the grid points in the box were successively discarded by grid filtering criteria.^[17] To generate the negative images of different sizes, we used five specific cutoff distances (4–12 Å by an increment of 2 Å). Seven chemical features (H-bond donor, H-bond acceptor, cation, anion, ring, hydrophobe, and hydroxyl group) were incorporated on the surface of the negative image based on the chemical features of atoms consisting of the binding pocket.^[28] Five chemical features (H-bond donor, H-bond acceptor, ring, hydrophobe, and hydroxyl group) were

assigned for each library compound (virtual ligand in this study). The SLIM-score between a compound i and a negative image is defined as the sum of their Z-transformed 3D shape similarity (S^{shape}) and chemical feature similarity (S^{CF}) values:

$$\text{SLIM-score}_i = S_{i,Z}^{\text{shape}} + S_{i,Z}^{\text{CF}} \quad (2)$$

S^{shape} is given by a Tanimoto coefficient calculated by the individual volumes and volume overlap between a negative image and a compound, each of which is represented by a Gaussian description of molecular shape.^[29] The volume overlap (VO) is defined as

$$VO_{\text{NC}} = \sum_{i \in \text{N}} \sum_{j \in \text{C}} p_i p_j \exp\left(-\frac{\alpha_i \alpha_j r_{ij}^2}{\alpha_i + \alpha_j}\right) \left(\frac{\pi}{\alpha_i + \alpha_j}\right)^{\frac{3}{2}} \quad (3)$$

where i and j are a grid point of a negative image (N) and an atom of a compound (C), respectively. p and α are the weight and exponent of a spherical Gaussian. r_{ij} is the distance between a grid point of a negative image (N) and an atom of a compound (C).

S^{CF} is defined as

$$S^{\text{CF}} = \sum_{i,j} \frac{1}{\exp(r_{ij})} \quad (4)$$

where r_{ij} is the distance between the assigned chemical features i (in a negative image) and j (in a compound). We calculated the chemical feature similarity only for pairs with distances $\leq 3 \text{ \AA}$, and only when their chemical features are identical, hydroxyl group (i) – H-bond donor/acceptor (j) and vice versa, cation (i) – H-bond donor (j), anion (i) – H-bond acceptor (j), and ring/hydrophobe (i) – ring/hydrophobe (j). Chemical feature assignments for library compounds and calculations of 3D shape and chemical feature similarity were performed by an in-house software written using Open Babel C++ library.^[26]

Benchmark Performance Evaluation

Compound sets consisting of actives and decoys (inactive compounds) for 40 and 102 protein targets were obtained from the Directory of Useful Decoys (DUD)^[30] and its enhanced version (DUD-E),^[31] respectively, to evaluate the high-throughput screening performance of crystal ligands, virtual ligands by *Stalis*, and a control docking tool, AutoDock Vina.^[14] The binding-site residues of each target were extracted from the provided crystal structure for each target using a cutoff distance of 5.0 \AA between any atoms of a protein residue and its cognate ligand (i.e., crystal ligand).

The DUD and DUD-E protein structures and compound sets were preprocessed using MGLTools (<http://mgltools.scripps.edu>, version 1.5) and Open Babel, respectively, for molecular docking using AutoDock Vina. Each docking box center was determined by the geometric center of the cognate ligand and the box size was set to 20 \AA in X, Y, and Z.

For each target, pairwise 2D similarities between its crystal ligand (or a virtual ligand) and DUD/DUD-E (active and decoy) compounds were quantified by a Tanimoto coefficient

calculated based on a path-based fingerprint (FPT) generated by Open Babel.^[32] Pairwise 3D shape similarities between a crystal ligand (or a virtual ligand) in a target protein and an ensemble of (active and decoy) compound structures were calculated by ROCS (Rapid Overlay of Chemical Structures, version 3.2)^[33]. An ensemble of up to 200 conformations of each compound was generated using the default parameters in the OMEGA program (version 2.5)^[34]. We used the ImplicitMillsDean color force field to measure chemical complementarity between compounds. The 3D similarity is given by the sum of the shape Tanimoto and scaled color values ranging from 0 to 2. All experiments were performed with default parameter values in ROCS.

The performance of *Stalis* was evaluated using the area-under-curve (AUC), enrichment factor (EF), and hit rate (HR). The AUC value is an objective measure of the overall performance of a given virtual screening tool in discriminating active compounds from decoy compounds. We plotted receiver operating characteristic (ROC) curves from the prediction results and calculated the AUC values. An AUC value of 1.0 indicates that the virtual screening tool perfectly prioritizes active compounds (i.e., an ideal case), while a value of 0.5 implies random prediction. EF describes the success of a virtual screening method at ordering the library with the active compounds to be screened first. Very high EF indicates that only a small percentage of the library needs to be screened to find a large number of active molecules. HR is a normalized expression of EF. EF and HR in the top $x\%$ of the screened library are defined as

$$EF^{x\%} = \frac{\text{No. of actives}^{x\%} / N_{\text{selected}}^{x\%}}{N_{\text{actives}} / N_{\text{total}}} \quad (5)$$

$$HR^{x\%} = \frac{EF_{\text{actual}}^{x\%}}{EF_{\text{ideal}}^{x\%}} \times 100 \quad (6)$$

For the performance evaluation of virtual ligands by *Stalis*, we used top five virtual ligands in this study. To use the multiple virtual ligands for ligand structure-based virtual screening, we used the unsupervised data fusion technique, where a final score is a weighted sum of the average and maximum score of the five virtual ligands.

$$\text{Score}_d = w \frac{\sum_{v=1}^{N_v} S(V_v | D_d)}{N_v} + (1-w) \max_{v \in (1, \dots, N_v)} [S(V_v, D_d)] \quad (7)$$

where N_v is the number of virtual ligands, $S(V, D)$ is a virtual screening score between a virtual ligand and a database compound, and w is an empirical weight parameter ($w = 0.2$).

Results

Development of Stalis

Stalis is an integrated method of *Stalis*^F and *Stalis*^W. *Stalis*^W uses ligand templates from a PDB library of whole (W) ligands and their binding sites. On the other hand, *Stalis*^F obtains the structure templates from a PDB library of ligand fragments (F) and their binding sites. Overall workflow of *Stalis*^W is schematically illustrated in Figure S5. (1) A set of binding sites with significant similarity (GA-score ≥ 0.6) to a target binding site is identified by G-LoSA from the PDB ligand/binding site library. (2) The template ligands in the identified binding sites are mapped onto the target binding site upon the structure superposition of their binding site. (3) Structurally similar ligand templates are excluded to remove the redundancy using a positional overlap Tanimoto coefficient (T_{PO}) with a cutoff of 0.7. T_{PO} is defined by $N_{OI}/(N_i + N_j + N_{OI})$, where N_{OI} , N_i , and N_j are the number of spatially overlapped identical atoms (only heavy atoms with distance ≤ 1.2 Å) between templates i and j , the total number of atoms in template i , and the total number of atoms in template j , respectively. Top 20 ligand templates are selected based on their GA-score from the non-redundant set. If GA-score is ≥ 0.7 , however, the templates are all selected regardless of the maximum template number. (4) Bad-contact atoms and non-interacting atom groups are removed from the template ligands. A bad-contact atom is defined by an atom overlap ratio with a cutoff of 0.5. The atom overlap ratio is defined by $(R_j + R_j - d_{ij})/(R_i + R_j)$, where i and j are atoms from a template ligand and a target protein, R is an atomic radius, and d_{ij} is a distance between atoms i and j . To identify non-interacting atom groups, each template ligand is dissected into fragments using *MolFrag*, and the fragments without any contacts from the target protein within 5.5 Å are removed from the template. (5) The trimmed templates are subject to druggability check by measuring number of atoms (the minimum number of atoms = 8 and the maximum number of atoms = 50) and number of rotatable bonds (the maximum number of rotatable bonds = 9).^[35] Remaining templates are filtered again using a T_{PO} cutoff of 0.5 to obtain more deserve non-redundant set. The top N templates, which is called “virtual ligands”, are selected from the set based on the GA-score.

Figure 4 schematically shows an overall workflow of *Stalis*^F. The workflow of *Stalis*^F is similar to that of *Stalis*^W, but has three major differences. (1) The first one is to use a PDB library of ligand fragments and their binding sites, instead of whole ligands and their binding sites. CFP-based iterative maximum clique search option is used for G-LoSA calculations. As in *Stalis*^W, top ligand fragment templates are selected based on their GA-scores from the non-redundant set. In *Stalis*^F, however, the maximum number of the top templates is set to 100 based on the abundance of the available templates due to their small size. (2) The second difference is the addition of fragment assembly step to generate larger molecules by linking neighboring fragments. The top templates are clustered by their spatial proximity (cutoff distance of 5.0 Å). The clusters are sorted by the best GA-score among the elements in each cluster. *Stalis*^F generates all possible assemblies using ligand fragment templates from different clusters when the fragment pair has less than two bad contacts. If the distance between bad-contact atoms is less than 0.7 Å, an end-atom (with only single linkage) between the two atoms is removed from the template. If the two atoms are both end-atoms, the chemical complementarity (hydrophobic, H-bond acceptor, H-bond donor, or hydroxyl

group) to their nearest receptor atoms are evaluated, and any atom with worse complementarity is removed from the template. The nearest atom pair between the ligand fragment templates are then identified within a distance range of 1–2 Å to assemble the two fragments. The maximum number of linkages that each atom can have are examined to check if the two templates could be assembled by adding a bond between the atoms (see Figure S6 for atom-deletion and fragment-assembly procedures). A generated fragment assembly is used as a new template to be assembled with another template during this fragment assembly step. This step is iterated to generate the maximum number of 50,000 fragment assemblies. (3) The last difference from *Stalis*^W is to use the SLIM-score^[17,28] to rapidly prioritize more reliable fragment assemblies. All ligand fragment templates and their assemblies are sorted by their SLIM-score, following druggability check and filtering using a T_{PO} cutoff of 0.5 to select top N virtual ligands. *Stalis* obtains top 20 virtual ligands separately from *Stalis*^W and *Stalis*^F. These virtual ligands are examined by the SLIM-score and then top N virtual ligands are finally chosen. All templates used in the top 20 virtual ligands by *Stalis*^F and *Stalis*^W for each DUD target are listed in Supporting Information List S1.

Benchmark performance validation

To evaluate the quality of virtual ligands generated by *Stalis*, we have carried out ligand structure-based virtual screening against 40 DUD and 102 DUD-E targets. The top five virtual ligands identified by *Stalis* were used as queries for fingerprint (FPT) calculations, a representative 2D ligand structure-based approach and ROCS calculations, a representative 3D ligand structure-based approach, against the (active and decoy) compound sets of the targets. We also examined the performance by combining FPT and ROCS (FPT+ROCS). The crystal ligand of each DUD/DUD-E target available in the websites (<http://dud.docking.org> and <http://dude.docking.org>, respectively) was also used as a query for the ligand structure-based virtual screening for performance comparison. As a control, we carried out molecular docking experiments using AutoDock Vina, a receptor structure-based virtual screening tool, for the compound sets of the targets. In *Stalis*, we excluded all the templates from homologous holo-proteins in our PDB libraries whose sequence identify is 30% to the target protein in order to remove the easy cases which could be detected by ligand (fragment) templates from homologous holo-proteins.

Table 1 reports the performances of virtual ligands by *Stalis* and crystal ligands in ligand structure-based virtual screening and AutoDock Vina in receptor structure-based virtual screening using the average AUC over the DUD and DUD-E targets and the number of targets whose AUC is ≥ 0.7 (a cutoff to evaluate success in virtual screening). The results show that simple combination of 2D and 3D ligand structure-based virtual screening methods increases the average AUC values in the DUD set, not in the DUD-E set due to the poor performance of ROCS. Combination of *Stalis*^F and *Stalis*^W improves the average AUC values in the DUD set or removes the ambiguity in selecting better method between *Stalis*^F and *Stalis*^W in the DUD-E set, showing their performance complementarity in designing virtual ligands in *Stalis*. In the DUD set, all *Stalis*-related approaches (*Stalis*^F, *Stalis*^W, and *Stalis* with FPT, ROCS, and FPT+ROCS) outperform AutoDock Vina, a control method for receptor structure-based virtual screening, in terms of both the average AUC and the number

of successful targets. The usage of crystal ligands for 2D and 3D ligand structure-based virtual screening shows better performance than all other approaches. When virtual ligands from *Stalis* are used for FPT+ROCS against the DUD targets, its performance (average AUC = 0.73 and the number of successful targets = 25) is comparable to those by each FPT (0.74 and 25) and ROCS (0.73 and 25) and slightly worse than that by FPT+ROCS (0.76 and 27) with the crystal ligands.

An AUC is a simple and convenient quantity to evaluate overall virtual screening performance, but this quantity has a limitation of characterizing ability to better identify more active compounds at the small fraction of screened compounds. As the complementary metrics of AUC, we measured EF (Table S1) and HR (Table 2) at top 1, 5, 10, 20, and 30% for the DUD set to further examine the performance of *Stalis*. The overall trend of the virtual screening performances measured by EF and HR is similar to that measured by AUC. However, the EF and HR tables report that ligand structure-based virtual screening using crystal ligands show better performance in particular at small fractions of screened compounds than using virtual ligands from *Stalis* (i.e., top 1, 5, and 10%). The results indicate that screening using *Stalis* virtual ligands needs more top-ranked screened compounds to identify the same number of active compounds than using crystal ligands, which results from the lower resolution of the virtual ligands. In *Stalis*, FPT shows much worse performance than ROCS at top 1%, eventually showing no improvement in EF and HT from the combination of FPT and ROCS. This suggests that *Stalis* virtual ligands are more effective to detect active compounds from small number of screened compounds through their 3D shape comparison in the case where the performance of ROCS is comparable to that of FPT. For all of the benchmark performance evaluations, we used the top five virtual ligands from *Stalis*^F, *Stalis*^W, and *Stalis*. Increase in the number of the virtual ligands did not show any improvement in the average performance (data not shown).

Similarity between crystal and virtual ligands and its relationship with performance in 2D FPT and 3D ROCS

Figure 5A shows the relationship of the best T_{PO} between top five *Stalis* virtual ligands and the crystal ligand for each of 40 DUD targets with the screening performance of the best virtual ligands in ROCS, measured by AUC (AUC_{ROCS}). The structural similarities of the best virtual ligands to their crystal ones show a modest positive correlation (Pearson correlation coefficient $r = 0.48$, $p < 0.05$) with the virtual screening performance, demonstrating that the performance of 3D ligand structure-based virtual screening is dependent to some extent on the *Stalis*' ability to accurately predict the structure of the native ligands. In Figure 6, we present four representative examples to illustrate the *Stalis*' ability to regenerate the native ligands. While the examples show significant structural similarity between the crystal ligands and best virtual ligands, the structure comparisons suggest that reliable prediction of the core structures of the native ligands determine the success of virtual ligands in 3D ligand structure-based virtual screening. The 2D FPT approach show less performance correlation with the structural similarity to the crystal ligands ($r = 0.36$, $p < 0.05$, data not shown), which results from the nature of its molecular fingerprint algorithm using atom-to-atom paths, requiring little to no 3D structure information. As expected, Figure 5B shows a weak correlation between 2D and 3D ligand

structure-based virtual screening performance ($r = 0.32$, $p < 0.05$), due to differences in their similarity calculation principles. Meanwhile, this also explains the origin of the performance improvement achieved by the combination of 2D and 3D approach (FPT+ROCS), shown in the benchmark evaluation results for the DUD set (Table 1). Representative examples are shown in Figure 7 to illustrate the performance complementarity between 2D FPT and 3D ROCS approach.

The screening performances of FPT are consistent over the DUD and DUD-E set, whereas ROCS shows much worse performances in the DUD-E set (Table 1). This decreased performance results from the less tolerance of ROCS to increased structural similarity between the active and decoy compounds in the DUD-E set,^[24,31] suggesting that 2D ligand structure-based approach works better with low-resolution ligands generated by *Stalis*.

Performance complementarity of *Stalis*^F and *Stalis*^W

We examined how many virtual ligands from *Stalis*^F are generated through assembly of multiple ligand fragments. In Figure 8, we plot the average number of fragments in top 20 virtual ligands from *Stalis*^F for the DUD set with respect to the number of binding-site residues. The plot shows a tendency that virtual ligands are made up with more ligand fragments as the target binding-site size is larger ($r = 0.49$, $p < 0.05$), indicating the ability of the fragment assembly step in *Stalis*^F to generate molecules that better fit into the target binding site.

Stalis selects five virtual ligands from top 20 virtual ligands separately from *Stalis*^F and *Stalis*^W. As shown in our benchmark performance evaluation results, this integration approach improves the performance of the virtual ligands in ligand structure-based screening, indicating their complementarity in designing better virtual ligands. We examined the five virtual ligands from *Stalis* to find out whether each virtual ligand comes from *Stalis*^F or *Stalis*^W. The result shows that average 3.83 and 3.39 virtual ligands over the 40 DUD and 102 DUD-E targets are generated by *Stalis*^F, respectively, indicating more dominant roles of *Stalis*^F in identifying better virtual ligands. Figure 9 shows the structures of crystal ligands and virtual ligands, where the screening performance of the virtual ligands by *Stalis*^F is largely different from that by *Stalis*^W in the DUD set, to illustrate the performance complementarity between both approaches.

Discussion and Conclusions

In this study, we have described a computational methodology, *Stalis* for ab initio ligand design by harnessing structure templates from the PDB libraries of whole ligands (*Stalis*^W) and their fragments (*Stalis*^F). Rather than identifying bioactive compounds from pre-existing compound libraries, *Stalis* generates a set of molecules whose structures represent the pocket shape and chemical features of a given target binding site. We have carried out a benchmark performance evaluation study to investigate how effective the designed molecules by *Stalis* (virtual ligands) are in computational screening of the 40 DUD and 102 DUD-E compound sets. The results show that computational ligand structure-based screening using *Stalis* virtual ligands outperforms receptor structure-based screening examined by a control molecular docking tool, AutoDock Vina. *Stalis* has comparable overall screening

performance to the case using crystal ligands in the DUD set. 2D ligand structure-based approach shows consistently reliable performance in both DUD and DUD-E set. Overall, the results demonstrate the reliable quality of *Stalis* virtual ligands and their applicability to ligand structure-based high-throughput virtual screening. Using crystal ligands as a query for ligand structure-based virtual screening, however, is the best approach over AutoDock Vina and *Stalis* particularly in identifying more active compounds at the small fraction of screened compounds. *Stalis* virtual ligands are worse in such ability due to the low-resolution of the computationally predicted molecular structures.

The most time-consuming step in *Stalis* is the G-LoSA search to identify binding sites that have similar geometry to a target binding site from the PDB structure libraries. However, based on the fact that G-LoSA has high computational speed (< 0.1 sec. for alignment of two ligand binding sites in general) and the PDB libraries can be easily divided into a number of small subsets on a high-performance computing system, *Stalis* is a computational methodology to promptly provide 3D structural information of ligands and their binding poses for a target protein. Given a target protein structure, we can define its potential ligand binding sites based on experimental data or using computational approaches such as our CMCS-BSP (Complementary Methods and Consensus Scoring for ligand Binding Site Prediction).^[36] Once a ligand binding site is determined, we can easily determine binding-site residues using the inner shape of the binding pocket. Given a target binding site consisting of the identified residues, we can apply *Stalis* to design virtual ligands and perform fast ligand structure-based virtual screening, eventually enabling to significantly downsize huge compound library. This screened small set of compound structures can be subject to computationally more expensive calculations including exhaustive docking using multiple receptor conformations and molecular dynamics simulations to finally select potential lead compounds. We believe that *Stalis* can greatly facilitate structure-based virtual screening campaigns. *Stalis* is also attractive in that this method provides actual 3D structures of molecules that likely bind to a target protein, making it possible to directly look at the structures and gain structural insight into potential ligands.

The major difference of *Stalis* from other available template-based methods is that our method identifies PDB ligand templates using local pocket alignment with G-LoSA, rather than using global structure alignments.^[28,37] Utilization of PDB ligand fragments in *Stalis*^F could further reduce the dependency of the template identification based on global structure similarity. To examine the potential merit of harnessing PDB ligand fragment/binding-site structure library, we performed additional benchmark performance evaluation by removing ligand templates from homologous PDB holo-proteins based on global structural similarity of the target to the library proteins using TM-align (TM-score cutoff = 0.4)^[38] as well as sequence identity. Indeed, FPT in *Stalis*^F shows a comparable performance to the case where templates from homologous holo-proteins are removed only based on the sequence identity (average AUC 0.66 to 0.67), while the *Stalis*^W performance decreases significantly (0.70 to 0.62) (Table 3). Despite this comparable performance of FPT in *Stalis*^F, the additional removal of templates by global structural similarity seems to lower the quality of virtual ligands generated as shown in the ROCS performance. The results also support higher tolerance of 2D ligand structure-based approach to the lower quality of virtual ligands.

Although *Stalis* shows reliable performance in ligand structure-based virtual screening, the methodology described in this study certainly has rooms to be improved for better performance. To illustrate our future direction, we evaluated *Stalis* performances with some prior knowledge (Table 4). If we selected better AUC between *Stalis*^F and *Stalis*^W and then calculated the average AUC over the 40 DUD targets, the performance improvement would be observed (0.75 w/ vs. 0.72 w/o prior knowledge for FPT and 0.74 w/ vs. 0.70 w/o prior knowledge for ROCS). As another case, if we calculated the average AUC using the best AUC values among top 10 virtual ligands from *Stalis* FPT+ROCS, the average AUC would become 0.82 with 34 successful targets (compared to 0.73 with 25 successful targets for top five virtual ligands w/o prior knowledge). The results of these ideal cases suggest that the *Stalis* performance in ligand structure-based virtual screening could be much more improved if better virtual ligands are selected from *Stalis*^F and *Stalis*^W. This imperfection of current *Stalis* might come from multiple factors including its algorithms for generating PDB structure libraries, aligning local structures by G-LoSA, assembling ligand fragment templates, and ranking virtual ligands by SLIM-score. We will continue to improve the algorithms in *Stalis* for its better performance.

Zhou *et al.* have recently reported an improved version of FINDSITE^{comb} (FINDSITE^{comb2.0}). FINDSITE^{comb2.0} identifies template proteins based on a SP3 threading, structure comparison, and structure-pocket comparison from multiple structure libraries built using the PDB, DrugBank, and ChEMBL database with advanced template selection algorithms.^[39] The method shows exceptional performance against the DUD-E set (average AUC=0.81), suggesting that templates identification through local/global combined structure similarity comparison, optimal filtering, and integration of available structural databases can significantly enhance the quality of virtual ligands.

With advances in computational methodologies for protein structure prediction, it is expected that complete 3D structural information of most proteins in an organism will become available soon. Therefore, it is a ripe time to develop efficient computational methods capable of harnessing the big biomolecular structure data to get proteomic-level insight into protein-ligand interactions. Moreover, rather than acting in isolation, the protein-ligand interactions usually carry out their biological processes through orchestration of complex networks of transient interactions. Therefore, proteome-scale approaches to protein-small molecule ligand interactions are imperatively needed to elucidate the fundamentals of complex biological systems and to develop more efficient therapeutic agents. We believe that *Stalis* could become a highly efficient computational platform for high-throughput ligand design at the proteomic level.

Supplementary Material

Refer to Web version on PubMed Central for supplementary material.

Acknowledgments

This work has been supported by NIH GM126140 and XSEDE MCB070009.

References

- [1]. Gerosa L, Sauer U, *Curr. Opin. Biotechnol* 2011, 22, 566. [PubMed: 21600757]
- [2]. Changeux JP, Christopoulos A, *Cell* 2016, 166, 1084. [PubMed: 27565340]
- [3]. Milroy LG, Grossmann LG, Hennig S, Brunsveld L, Ottmann C, *Chem. Rev* 2014, 114, 4695. [PubMed: 24735440]
- [4]. Tagore R, Thomas HR, Homan EA, Munawar A, Saghatelian A, *J. Am. Chem. Soc* 2008, 130, 14111. [PubMed: 18831549]
- [5]. Mayr LM, Bojanic D, *Curr. Opin. Pharmacol* 2009, 9, 580. [PubMed: 19775937]
- [6]. Scott DE, Coyne AG, Hudson SA, Abell C, *Biochemistry* 2012, 51, 4990. [PubMed: 22697260]
- [7]. Scannell JW, Blanckley A, Boldon H, Warrington B, *Nat. Rev. Drug Discov* 2012, 11, 191. [PubMed: 22378269]
- [8]. Kitchen DB, Decornez H, Furr JR, Bajorath J, *Nat. Rev. Drug Discov* 2004, 3, 935. [PubMed: 15520816]
- [9]. Pagadala NS, Syed K, Tuszynski J, *Biophys. Rev* 2017, 9, 91. [PubMed: 28510083]
- [10]. Jones G, Willett P, Glen RC, Leach AR, Taylor R, *J. Mol. Biol* 1997, 267, 727. [PubMed: 9126849]
- [11]. Schapira M, Abagyan R, Totrov M, *J. Med. Chem* 2003, 46, 3045. [PubMed: 12825943]
- [12]. Jain AN, *J. Med. Chem* 2003, 46, 499. [PubMed: 12570372]
- [13]. Friesner RA, Banks JL, Murphy RB, Halgren TA, Klicic JJ, Mainz DT, Repasky MP, Knoll EH, Shelley M, Perry JK, Shaw DE, Francis P, Shenkin PS, *J. Med. Chem* 2004, 47, 1739. [PubMed: 15027865]
- [14]. Trott O, Olson AJ, *J. Comput. Chem* 2010, 31, 455. [PubMed: 19499576]
- [15]. Allen WJ, Balias TE, Mukherjee S, Brozell SR, Moustakas DT, Lang PT, Case DA, Kuntz ID, Rizzo RC, *J. Comput. Chem* 2015, 36, 1132. [PubMed: 25914306]
- [16]. Murray CW, Baxter CA, Frenkel AD, *Comput J. Aided Mol. Des* 1999, 13, 547.
- [17]. Lee HS, Lee CS, Kim JS, Kim DH, Choe H, *J. Chem. Inf. Model* 2009, 49, 2419. [PubMed: 19852439]
- [18]. Sheng C, Zhang W, *Med. Res. Rev* 2013, 33, 554. [PubMed: 22430881]
- [19]. Berman HM, Westbrook J, Feng Z, Gilliland G, Bhat TN, Weissig H, Shindyalov IN, Bourne PE, *Nucleic Acids Res.* 2000, 28, 235. [PubMed: 10592235]
- [20]. Lee HS, Im W, *J. Chem. Inf. Model* 2012, 52, 2784. [PubMed: 22978550]
- [21]. Lee HS, Im W, In *Methods in Molecular Biology: Protein Function Prediction*; Kihara D, Ed.; Springer, 2017.
- [22]. Lee HS, Im W, *Protein Sci.* 2016, 25, 865. [PubMed: 26813336]
- [23]. Moriaud F, Doppelt-Azeroual O, Martin L, Oguievetskaia K, Koch K, Vorotyntsev A, Adcock SA, Delfaud F, *J. Chem. Inf. Model* 2009, 49, 280. [PubMed: 19434830]
- [24]. Roy A, Srinivasan B, Skolnick J, *J. Chem. Inf. Model* 2015, 55, 1757. [PubMed: 26225536]
- [25]. Govindaraj RG, Brylinski M, *BMC Bioinformatics* 2018, 19, 91. [PubMed: 29523085]
- [26]. O'Boyle NM, Banck M, James CA, Morley C, Vandermeersch T, Hutchison GR, *J. Cheminform* 2011, 3, 33. [PubMed: 21982300]
- [27]. Hanser T, Jauffret P, Kaufmann G, *J. Chem. Inf. Comput. Sci* 1996, 36, 1146.
- [28]. Lee HS, Zhang Y, *Proteins* 2012, 80, 93. [PubMed: 21971880]
- [29]. Grant JA, Gallardo MA, Pickup BT, *J. Comp. Chem* 1996, 14, 1653.
- [30]. Huang N, Shoichet BK, Irwin JJ, *J. Med. Chem* 2006, 49, 6789. [PubMed: 17154509]
- [31]. Mysinger MM, Carchia M, Irwin JJ, Shoichet BK, *J. Med. Chem* 2012, 55, 6582. [PubMed: 22716043]
- [32]. Willett P, *Drug Discov. Today* 2006, 11, 1046. [PubMed: 17129822]
- [33]. ROCS, OpenEye Scientific Software, Inc., Santa Fe, NM.
- [34]. OMEGA, OpenEye Scientific Software, Inc., Santa Fe, NM.
- [35]. Daina A, Michielin O, Zoete V, *Sci. Rep* 2017, 7, 42717. [PubMed: 28256516]

- [36]. Lee HS, Im W, J. Chem. Inf. Model 2013, 53, 2462. [PubMed: 23957286]
- [37]. Brylinski M, Skolnick J, Proc. Natl. Acad. Sci. U. S. A 2008, 105, 129. [PubMed: 18165317]
- [38]. Zhang Y, Skolnick J, Nucleic Acids Res. 2005, 33, 2302. [PubMed: 15849316]
- [39]. Zhou H, Cao H, Skolnick J, J. Chem. Inf. Model 2018, 58, 2343. [PubMed: 30278128]

Author Manuscript

Author Manuscript

Author Manuscript

Author Manuscript

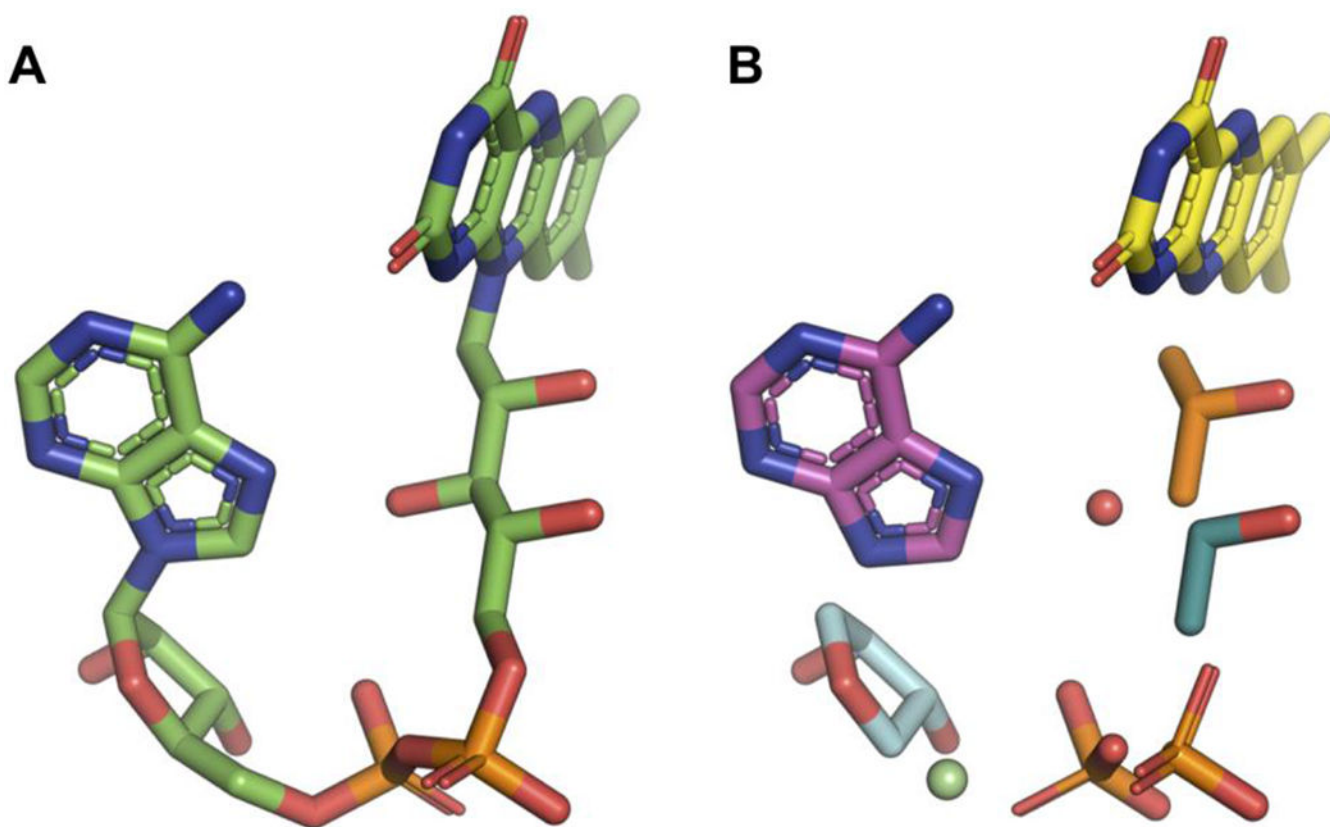


Figure 1.
Example of fragmentation of a PDB ligand (ligand FAD in PDB 1a8p) by *MolFrag*.

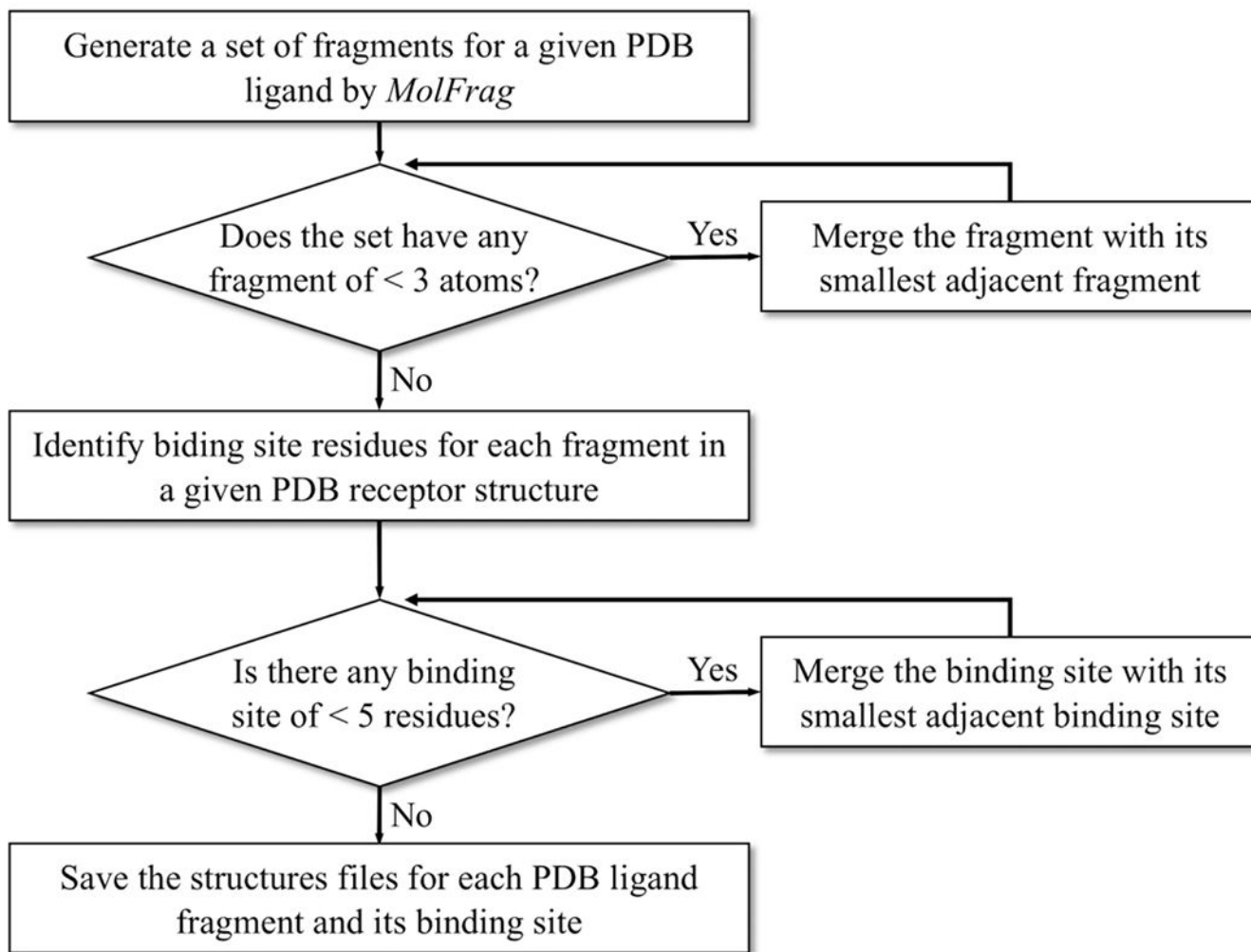


Figure 2. Workflow of generating a PDB binding-site library using the ligand fragments generated using *MolFrag*.

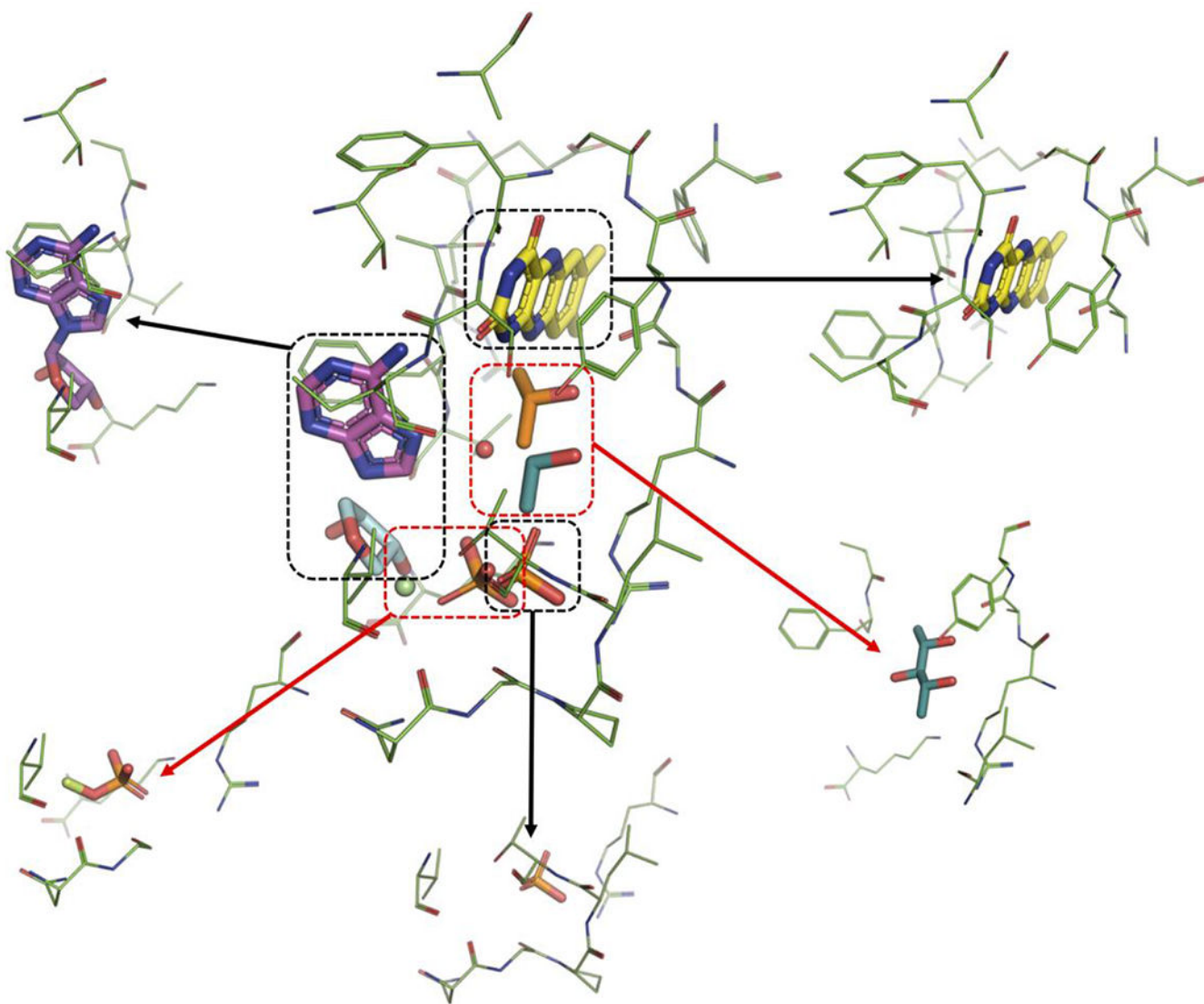


Figure 3. Procedure of binding-site identification for the ligand fragments by *MolFrag* in Figure 1.

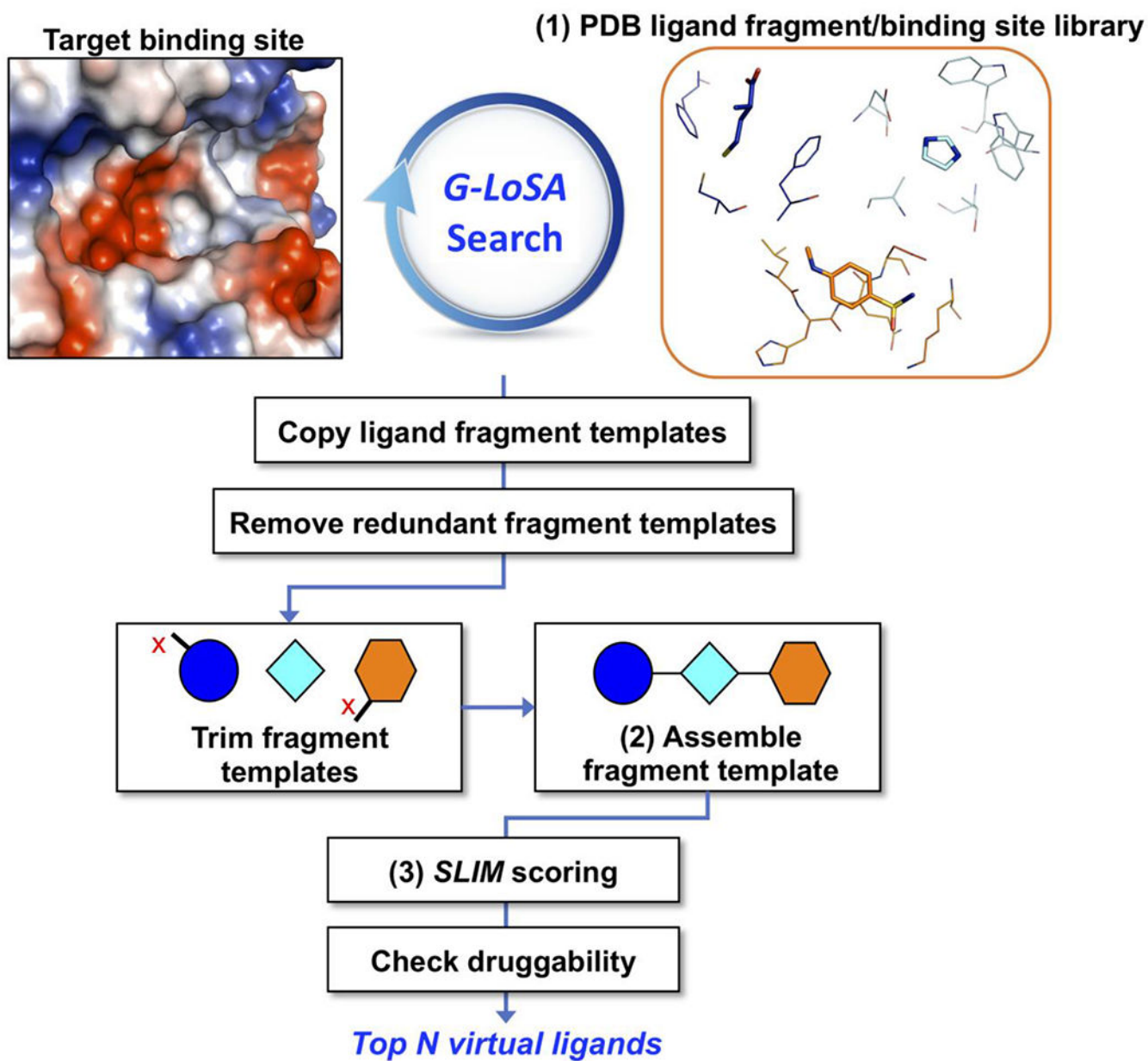


Figure 4. Schematic illustration of *Stalis*^F workflow. Numbers in parenthesis indicate that these steps are elaborated in the Results section.

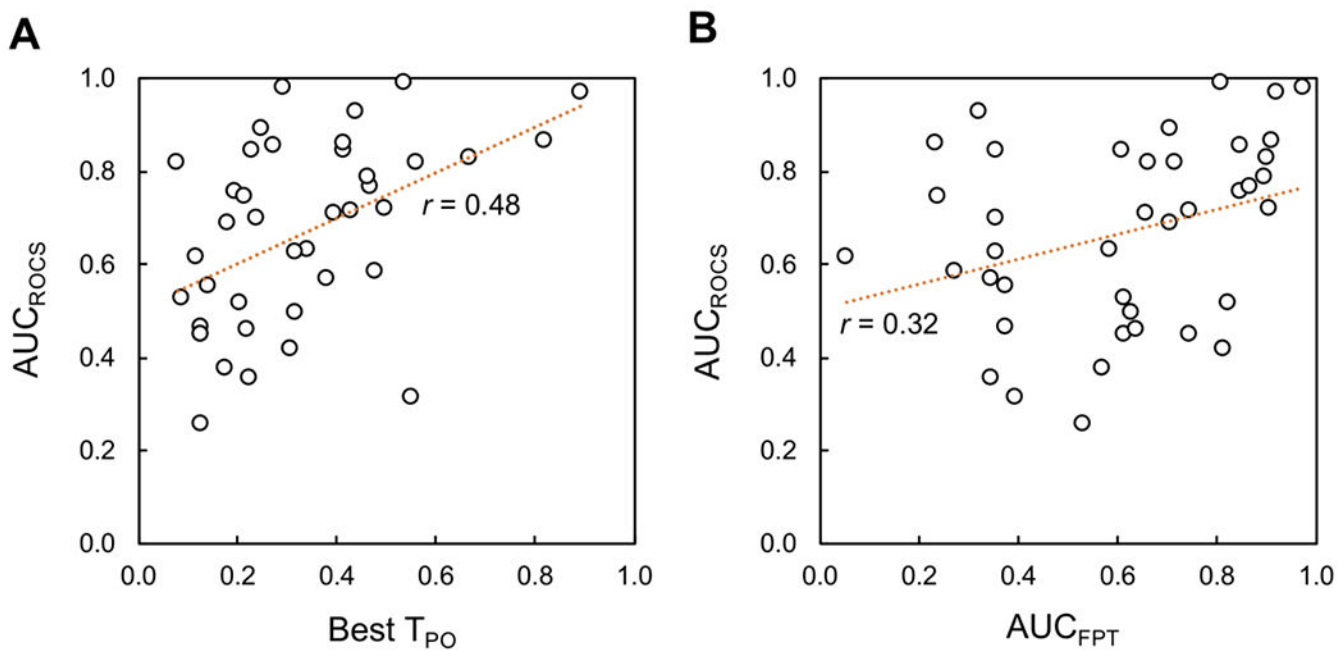


Figure 5. Similarity between virtual and crystal ligands and its relationship with performance in 2D FPT and 3D ROCS. (A) Relationship of the best T_{PO} (between top five virtual ligands generated by *Stalis* and the crystal ligands for 40 DUD targets) with the screening performance of the best virtual ligands in ROCS, measured by AUC (AUC_{ROCS}). (B) Relationship of the screening performance of the best virtual ligands in FPT (AUC_{FPT}) with that in ROCS (AUC_{ROCS}).

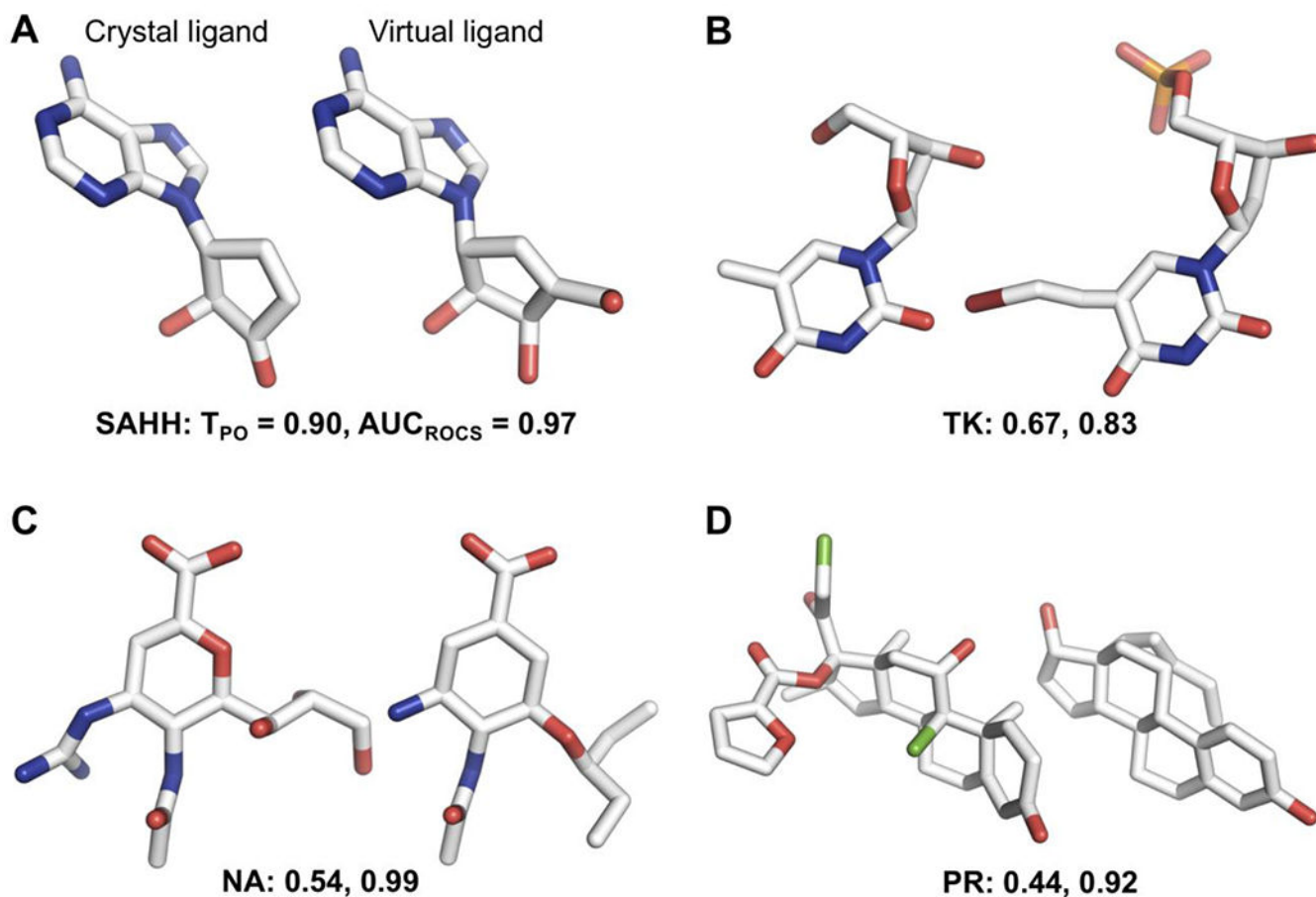


Figure 6. Representative examples to illustrate the *Stalis'* ability to regenerate the native ligands. The virtual ligands were selected from Figure 5A. The pairs of crystal ligand and virtual ligand for four DUD targets [(A) SAHH, (B) TK, (C) NA, and (D) PR] are shown with their T_{PO} and average AUC by ROCS (AUC_{ROCS}). All of the crystal and virtual ligands are receptor-bound structures, but the receptor structures are not shown for clarity. PDB IDs for the crystal ligands and PDB templates used in the virtual ligands are shown in Figure S7.

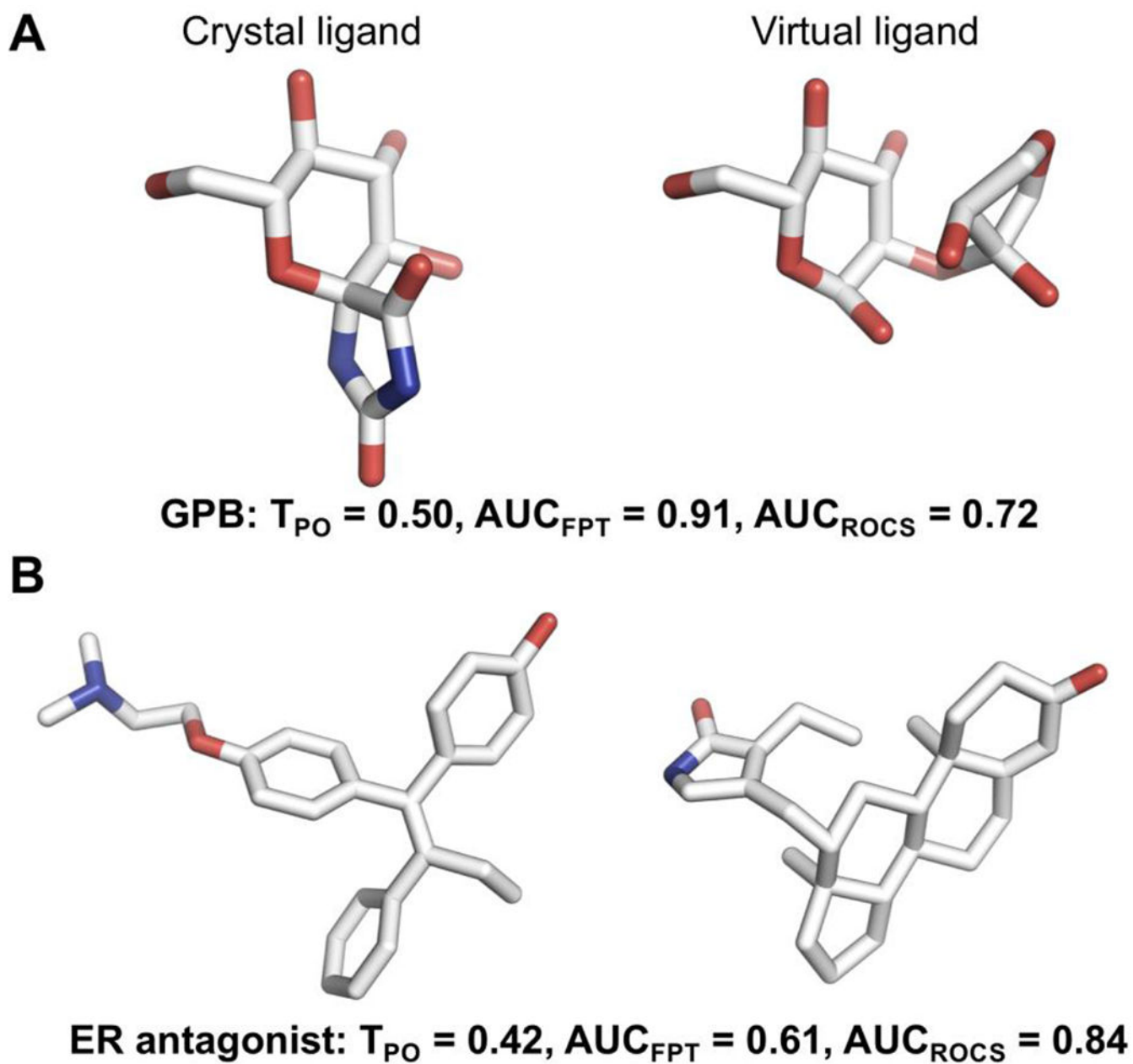


Figure 7.

Representative examples to illustrate the performance complementarity between 2D FPT and 3D ROCS approach. The virtual ligands were selected from Figure 5B. The pairs of crystal ligand and virtual ligand for two DUD targets [(A) GPB and (B) ER antagonist] are shown with their T_{PO} , average AUC by FPT (AUC_{FPT}), and average AUC by ROCS (AUC_{ROCS}). PDB templates used in the virtual ligands are shown in Figure S8.

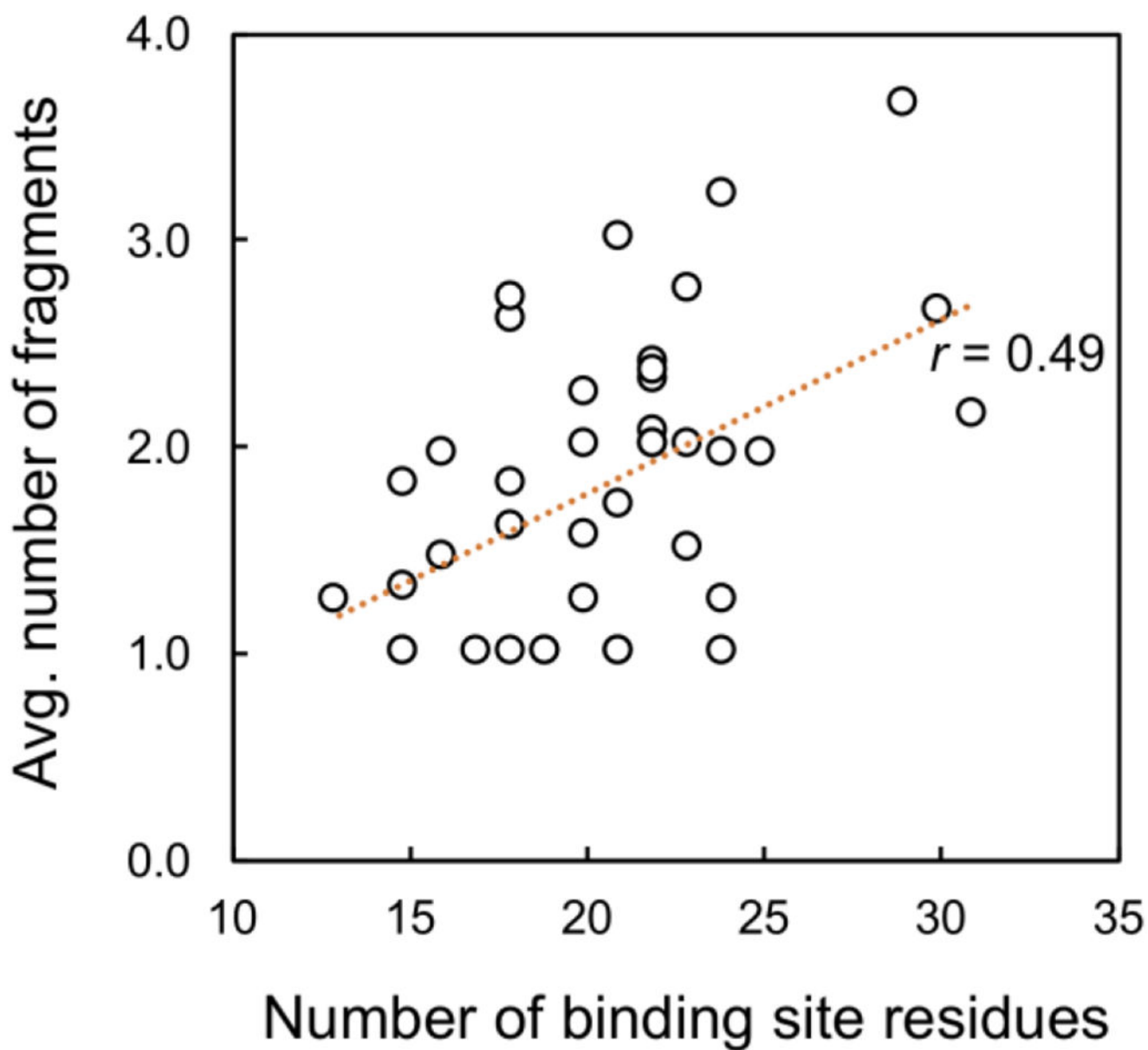


Figure 8. Relationship of the average number of fragments in top 20 virtual ligands from *Stalis*^F with respect to the number of binding site residues.

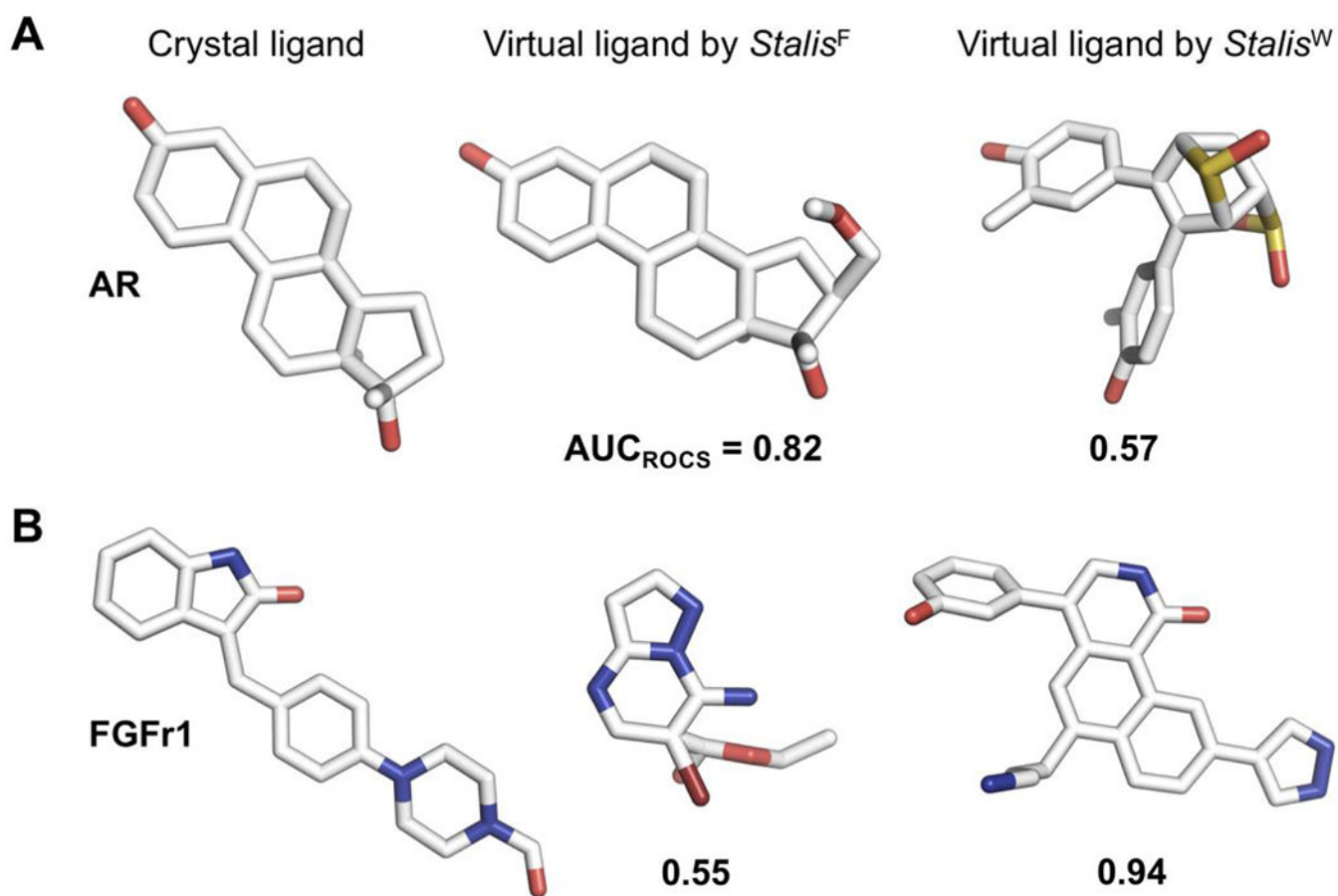


Figure 9. Representative examples to illustrate the performance complementarity between *Stalis*^F and *Stalis*^W. For this illustration, we divided top five virtual ligands by *Stalis* into virtual ligands from *Stalis*^F and those from *Stalis*^W, and then selected representative virtual ligands showing large performance difference in the average AUC by ROCS for two DUD targets [(A) AR and (B) FGFr1]. PDB templates used in the virtual ligands are shown in Figure S9.

Table 1.

Virtual screening performance of different receptor or ligand structure-based virtual screening methods against 40 DUD targets, measured using the average AUC and the number of successful targets.

Ligand	Method	DUD (40 targets)		DUD-E (102 targets)	
		Average AUC	# Targets of AUC ≥ 0.7	Average AUC	# Targets of AUC ≥ 0.7
	AutoDock Vina	0.62 \pm 0.16	14	0.69 \pm 0.13	55
Crystal ligand	FPT	0.74 \pm 0.18	25	0.76 \pm 0.13	67
	ROCS	0.73 \pm 0.20	25	0.70 \pm 0.15	59
	FPT+ROCS ^a	0.76 \pm 0.18	27	0.77 \pm 0.14	76
Virtual ligands by <i>Stalis</i> ^F	FPT	0.68 \pm 0.18	21	0.66 \pm 0.15	44
	ROCS	0.69 \pm 0.18	25	0.52 \pm 0.18	19
	FPT+ROCS	0.71 \pm 0.17	23	0.60 \pm 0.18	32
Virtual ligands by <i>Stalis</i> ^W	FPT	0.67 \pm 0.22	19	0.70 \pm 0.17	60
	ROCS	0.67 \pm 0.21	21	0.57 \pm 0.18	26
	FPT+ROCS	0.70 \pm 0.22	24	0.66 \pm 0.19	46
Virtual ligands by <i>Stalis</i>	FPT	0.72 \pm 0.18	22	0.69 \pm 0.17	55
	ROCS	0.70 \pm 0.19	25	0.56 \pm 0.19	26
	FPT+ROCS	0.73 \pm 0.18	25	0.65 \pm 0.20	45

^aIn the FPT+ROCS approach, the final virtual screening score for each DUD compound is the sum of its FPT score (FPT score range: 0–1) and the half of its ROCS score (ROCS score range: 0–2).

Table 2.

Virtual screening performance of different receptor or ligand structure-based virtual screening methods against 40 DUD targets, measured using the average HR in the top $x\%$ of the screened library. The standard deviations are not included in the table for clarity.

Ligand	Method	HR ^{1%}	HR ^{5%}	HR ^{10%}	HR ^{20%}	HR ^{30%}
	AutoDock Vina	19.23	20.50	28.71	40.47	49.35
Crystal ligand	FPT	53.37	42.18	49.66	57.83	65.17
	ROCS	55.78	42.10	50.30	58.67	65.08
	FPT+ROCS	58.12	46.66	54.26	62.76	69.62
Virtual ligands by <i>Stalis</i> ^F	FPT	16.09	17.95	28.83	45.94	57.97
	ROCS	30.47	23.56	33.83	48.79	60.88
	FPT+ROCS	21.52	23.50	33.96	49.42	60.65
Virtual ligands by <i>Stalis</i> ^W	FPT	21.35	23.14	36.21	46.33	55.06
	ROCS	33.22	28.67	37.73	47.17	54.58
	FPT+ROCS	28.08	28.12	37.97	51.67	61.68
Virtual ligands by <i>Stalis</i>	FPT	22.76	23.67	36.01	52.95	63.64
	ROCS	34.64	27.67	37.91	51.34	62.08
	FPT+ROCS	29.91	29.36	38.38	53.90	64.50

Table 3.

Virtual screening performance for the DUD set by removing PDB ligand templates based on global structural similarity of the target to the library proteins using TM-align as well as sequence identity.

Ligand	Method	Average AUC	# Targets of AUC ≥ 0.7
Virtual ligands by <i>Stalis</i> ^F	FPT	0.69 \pm 0.16	22
	ROCS	0.57 \pm 0.20	11
	FPT+ROCS	0.66 \pm 0.16	17
Virtual ligands by <i>Stalis</i> ^W	FPT	0.62 \pm 0.20	15
	ROCS	0.59 \pm 0.20	12
	FPT+ROCS	0.64 \pm 0.21	17
Virtual ligands by <i>Stalis</i>	FPT	0.70 \pm 0.15	21
	ROCS	0.57 \pm 0.19	12
	FPT+ROCS	0.67 \pm 0.17	18

Table 4.

Virtual screening performance in two ideal cases. One case “Better AUC between *Stalis*^F and *Stalis*^W” means that we select better AUC between *Stalis*^F and *Stalis*^W and then calculate the average AUC over the 40 DUD targets. The other case “Best AUC among top 10 virtual ligands from *Stalis*” means that we calculate the average AUC using the best AUC values among top 10 virtual ligands from *Stalis*.

Description	Method	Average AUC	# Targets of AUC ≥ 0.7
Better AUC between <i>Stalis</i> ^F and <i>Stalis</i> ^W	FPT	0.75 \pm 0.16	26
	ROCS	0.74 \pm 0.18	29
Best AUC among top 10 virtual ligands from <i>Stalis</i>	FPT+ROCS	0.82 \pm 0.14	34

Author Manuscript

Author Manuscript

Author Manuscript

Author Manuscript